APPLIED PHYSICS LETTERS 95, 263703 (2009)

Three dimensional microstructuring of biopolymers by femtosecond laser irradiation

M. Oujja,[1] S. Pérez,[1] E. Fadeeva,[2] J. Koch,[2] B. N. Chichkov,[2] and M. Castillejo[1,a)]
[1]*Instituto de Química Física Rocasolano, CSIC, Serrano 119, 28006 Madrid, Spain*
[2]*Laser Zentrum Hannover e.V., Hollerithallee 8, D-30419 Hannover, Germany*

(Received 16 July 2009; accepted 21 November 2009; published online 31 December 2009)

A sequence of single femtosecond pulses is used to create a pattern of laser affected spots at increasing depths below the surface of transparent biopolymer samples. Materials with different water contents and mechanical strengths, gelatine, chitosan, synthetic polyvinyl pyrrolidone, and biopolymer-polymer blends, are irradiated near the edge of the sample with an amplified Titanium:Sapphire laser (800 nm) delivering 30 fs pulses through a 0.45 numerical aperture objective with energies of 100–3000 nJ. The micrometric modified region is observed by optical microscopy perpendicularly to irradiation. Self-focusing and optical aberration are major factors controlling morphology and size of the created spots. © *2009 American Institute of Physics*. [doi:10.1063/1.3274127]

Fabrication of micro- and nanostructures on biocompatible materials is of high interest in technological areas of organic photonics and biomedicine.[1–4] Chemically active artificial two/three dimensions scaffolds with structures of defined form, dimensions and separation, giving rise to controlled substrate characteristics, can be used to adapt cell growth and functionality.[2] At present, common simple, low-cost tools applicable to bioengineering are usually based on methods used in microelectronics, however, the typical incompatibility of biomaterials with standard microfabrication techniques has stimulated the search for alternative approaches. Those exploited in the past 15 years for nanostructure fabrication of organic materials include microcontact printing,[5] nanoimprint lithography,[6] and laser-based methods[4,7,8] which allow good versatility and reliability in high-resolution patterning on these materials.[9]

Recently femtosecond (fs) laser nanostructuring is being considered as a viable method to process, fabricate, and customize materials for use in organic photonics and electronics, medicine, and bioengineering.[10] Femtosecond multipulse irradiation at MHz repetition rates and pulse energies of the order of nJ focused through a microscope objective can be used to achieve high-precision submicrometer scale modifications in polymers and biological tissues.[11–14] If sufficiently high numerical apertures (NA) are used, the focus diameter is reduced and unwanted nonlinear effects leading to filamentation and streak formation can be avoided; at the same time the nonlinear absorption allows the production of precisely localized modified areas of submicrometer dimensions inside the bulk of transparent materials.[15,16] In addition to bulk structuring, some examples of superficial fs laser processing of biopolymers and polymer-biopolymer blends have been reported.[17–19]

A number of natural polymers, such as gelatine, chitosan, and others, are being employed as biomaterials as they offer the advantage of being similar to macromolecular substances, which the biological environment is prepared to recognize and to deal with metabolically. Useful properties, i.e., improved resistance to degradation by naturally occurring enzymes, can be obtained by blending natural and synthetic polymers.[20]

In the present study, sequences of 800 nm, 30 fs pulses are used to create a pattern of laser affected spots with micrometer dimensions at increasing depths below the surface in samples of transparent polymers and biopolymers with different water contents and mechanical properties, such as gelatine, chitosan, synthetic polyvinyl pyrrolidone polymer (PVP), and of biopolymer-polymer blends. The effects of self-focusing and optical aberration are discussed as major factors that control the morphology of the laser created spots inside the material.

Gelatine is a protein obtained by denaturation of collagen involving the destruction of the tertiary and secondary structures. This biopolymer has served in previous laser ablation studies as model substance for soft biological tissue since it has absorption spectra and dielectric properties comparable to those of living material.[18,19] Chitosan is a linear polysaccharide composed of randomly distributed β-(1–4)-linked D-glucosamine (deacetylated unit) and N-acetyl-D-glucosamine (acetylated unit). It is a nontoxic, biodegradable, and biocompatible material, produced commercially from chitin, structural element in exoskeleton of crustaceans.[21] PVP, $(C_6H_9NO)_n$, is a chemically inert, and biocompatible synthetic polymer used for the preparation of synthetic plasmas and thromboresistant hydrophilic gels.[22] While gelatine is an amorphous material, both chitosan and PVP are crystalline. In the quest for development of advanced biomaterials, the properties PVP-biopolymer blends have been the subject of several studies.[22,23] Mixtures of chitosan and PVP are no longer crystalline as both polymer chains form a miscible phase that prevents crystallization of the individual polymers.[23]

Transparent films of the different materials, about 1 mm thick, were prepared by solvent evaporation and cast on petri dishes for 8 h. Samples of $10\times10\ \text{mm}^2$ were cut and the thin edges were finished using a microtome (LEICA RM2155). Gelatine (gel strength value B225) and PVP samples were prepared at 37 °C from aqueous solutions (6.67 wt %). For chitosan and chitosan-PVP blend (at 50% weight) the solvent was acetic acid (0.4 mol). All compounds

---

[a)] Electronic mail: marta.castillejo@iqfr.csic.es. Tel.: +34-91-7459515.

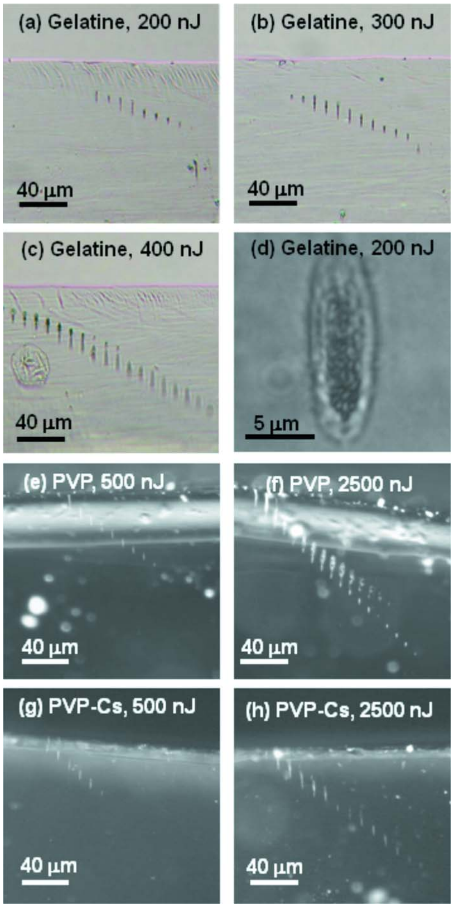

FIG. 1. (Color online) Side view optical microscopy images of features produced in bulk materials at increasing depths by single 30 fs laser pulses focused at 0.45-NA in: (a) gelatine, 200 nJ, (b) gelatine, 300 nJ, (c) gelatine, 400 nJ, (e) PVP, 500 nJ, (f) PVP, 2500 nJ, (g) PVP-chitosan (PVP-Cs) blend, 500 nJ and (h) PVP-chitosan blend, 2500 nJ. The picture in (d) is an enlarged view of a single feature in (a). The laser beam is incident from the top of the figures.

were supplied by Aldrich Chemicals. Once prepared, the samples were inspected by optical microscopy in order to ensure sufficiently flat surfaces for laser exposure. Samples were processed with an amplified Titanium:Sapphire laser (Femtopower compact Pro) delivering a 1 kHz train of 800 nm, 30 fs pulses. Computer control allowed delivery of single pulses from the laser with energies at the sample in the 100–3000 nJ range. The laser beam, with Gaussian profile of quality factor $M^2=1.2$, was tightly focused through a 50× microscope objective (Nikon, working distance=13.8 mm, NA=0.45) inside the samples placed on a submicrometer resolution XYZ translator stage. The voxels were observed perpendicularly to the irradiation using a Leica 1500 LCD microscope (160×) equipped with a digital camera.

Figures 1(a)–1(c) show optical microscopy images of the arrays of voxels created in gelatine using energies per pulse of 200, 300, and 400 nJ. Each spot is generated by a single laser pulse focused at increasingly larger depths in steps of 4 μm. For this material the energy threshold for damage at 0.45-NA is 150 nJ. Similarly Figs. 1(e)–1(h) display structures created in PVP and in PVP-chitosan blend. By increasing the pulse energy it is possible to create more structures at larger depths as represented in Fig. 2. However, above ≈2500 nJ the reachable depth is limited, preventing the fabrication of deeper structures in the bulk. The highest depth reached by fs microstructuring was around 180 μm in PVP.

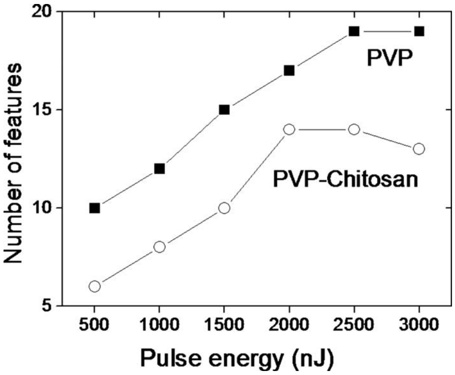

FIG. 2. Evolution of the number of features with pulse energy created inside the bulk of PVP and PVP-chitosan blend by single 30 fs laser pulses focused at 0.45-NA.

The features show an elongated shape along the laser propagation direction, with lateral dimension around 2–4 μm and length in the range of 10–40 μm. These dimensions increase with depth and laser pulse energy. It is also noticed that the shape of the features evolves from a cylinder structure, Fig. 1(d), to a jetlike shape as the laser aims at larger depths. It was found that for a given pulse energy, PVP features are the largest, followed by those in PVP-chitosan and gelatine.

The size of the structures can be compared with the dimensions of the laser focus.[15,24] For a Gaussian beam the waist of the focal spot is given by

$$\varpi_0 = \frac{0.61 M^2 \lambda_0}{n_0 NA}, \tag{1}$$

where λ_0 and n_0 are the laser wavelength and the refractive index of the media respectively. The confocal parameter of the Gaussian beam, or doubled Rayleigh length, the focal spot area and volume are given by

$$2z_R = 2\frac{\pi\varpi_0^2}{M^2\lambda_0}n_0, \tag{2}$$

$$S_{1/2} = 0.405\frac{M^4\lambda_0^2}{NA^2}, \tag{3}$$

$$V_{1/2} = 2z_R S_{1/2}^2 = 0.947\frac{M^6\lambda_0^3}{NA^4}n_0. \tag{4}$$

The peak laser power is approximated by $I_0=E_0/2t_pS_{1/2}$ with E_0 the pulse energy and t_p the pulse duration. Table I summarizes the focusing conditions of experiments herein.

The position below the surface and the shape of the structures are affected by self-focusing and distortion of the focal light intensity distribution due to spherical aberration. The self-focusing power threshold, P_{cr}, depends on the nonlinear part of refractive index, n_2, as $P_{cr}=\lambda_0^2/2\pi n_0 n_2$ and is calculated (Table I) by approximating the nonlinear refractive index of the material studied here by that of water.[25] At the working pulse energies, the laser power is above the critical value for self-focusing, as revealed by the elongated shape of the observed features which are longer than the calculated confocal parameter (Table I). On the other hand, the observed evolution of shape with depth is related to changes in the focal intensity distribution with the distance from the surface due to optical aberrations.[15]

TABLE I. Biopolymer and polymer parameters and focusing conditions for laser irradiation at 800 nm, 30 fs, 0.45-NA.

Material	Gelatine	PVP	Chitosan
n_0	1.33	1.45	1.58
n_2 (cm^2/W) [a]	5.7×10^{-16}	5.7×10^{-16}	5.7×10^{-16}
P_{cr} (MW)	1.3	1.2	1.1
ω_0 (μm)	0.96	0.90	0.81
$2z_R$ (μm)	5.6	5.1	4.7
$S_{1/2}$ (μm^2)	1.8	1.8	1.8
$V_{1/2}$ (μm^3)	14.9	13.6	12.6
$I_0/2$ (in W/cm^2 for 100 nJ)	9×10^{13}	9×10^{13}	9×10^{13}
P (in MW for 100 nJ)	3.3	3.3	3.3
T_g (°C)	187[b]	155[c]	203[c]
Young modulus (MPa)	5–10[d]	1187[e]	800[e]

[a] Reference 25.
[b] Reference 26.
[c] Reference 23.
[d] Reference 27.
[e] Reference 28.

As discussed by other authors[11,15,29] laser induced breakdown is the responsible mechanism for the generation of voxels in the bulk of the transparent polymeric materials studied herein. This process is described in terms of the creation of plasma of quasi free electrons by multiphoton and impact ionization and the subsequent transfer of the plasma energy to the lattice. The morphology of an individual voxel, Fig. 1(d), is well interpreted by the expansion of the dense plasma that creates a low density area surrounded by a region of compressed material. Chemical effects taking place in the free electron plasma can be discussed in terms the fragmentation of the organic molecular solid initiated by capture of electrons into antibonding orbitals and, in the case of materials with water content (4% in gelatine) by ionization and dissociation of water molecules.[12] These effects would contribute to the generation of gaseous products inside the voxels. Additionally, generated free radicals and reactive oxygen species can initiate the oxidation and reduction of the organic material. In gelatine, it has been observed that laser irradiation induces the photo-oxidation of the side chain of the aromatic amino acid tyrosine in dytirosine.[18,30] Similar effects could be responsible of a partial degradation of the material on the inner surface of the generated structures.

On the other hand, the observed evolution of the shape of voxels from cylindrical to conical, also reported in other type of dielectrics,[31] are attributed to the different temporal slices of the pulse producing breakdown at different positions of the material. The differences in voxel size and depth of accessible region observed in the different materials are explained in reference to their mechanical and thermal properties (Table I). In fact, as shown, the reachable depth and size of microstructures follows the trend of the Young's modulus, with PVP having the larger values.

In conclusion, arrays of micrometer size features up to 180 μm below the surface of transparent bulk gelatine, chitosan, PVP, and PVP-chitosan blends were fabricated by a sequence of 800 nm, 30 fs pulses focused at 0.45-NA and pulse energies in the 100–3000 nJ range. The depth of the created features coincides with the aimed depth but their morphology evolves from a cylinder at shallow depths to a jetlike type at larger ones. This is explained by the effect of self-focusing and by the influence of optical aberrations that modify the intensity profile with depth. While these effects can be compensated by operating at larger NAs, the differences in mechanical and thermal properties of the biocompatible materials give account of the differences in size and reachable depth of the micrometric structures. Further research aims at the full characterization of the material inside the created features and the possible detrimental implications for biomedical applications, as the results shown open the possibility of using cheap, biocompatible polymers and biopolymers in cutting edge applications in photonics and biotechnology (i.e., drug release, tissue engineering).

Funding from Project No. CTQ2007-60177, Spain is gratefully acknowledged. M.C. thanks Dr. S. Lazare for useful discussions and S.P. MICINN, Spain, for a FPI fellowship.

[1] C. Paquet and E. Kumacheva, Mater. Today **11**, 48 (2008).
[2] D. W. Wilkinson, M. Riehle, M. Wood, J. Gallagher, and A. S. G. Curtis, Mater. Sci. Eng., C **19**, 263 (2002).
[3] A. Ovsianikov, A. Ostendorf, and B. N. Chichkov, Appl. Surf. Sci. **253**, 6599 (2007).
[4] J. G. Fernandez, C. A. Mills, and J. Samitier, Small **5**, 614 (2009).
[5] Y. Xia and G. M. Whitesides, Annu. Rev. Mater. Sci. **28**, 153 (1998).
[6] S. Y. Chou, P. R. Krauss, and P. J. Renstrom, Appl. Phys. Lett. **67**, 3114 (1995).
[7] H. Y. Zheng, T. T. Tan, and W. Zhou, Opt. Lasers Eng. **47**, 180 (2009).
[8] C. A. Aguilar, Y. Lu, S. I. Mao, and S. Chen, Biomaterials **26**, 7642 (2005).
[9] M. Cecchini, G. Bumma, M. Serresi, and F. Beltram, Nanotechnology **18**, 505103 (2007).
[10] *3D Laser Microfabrication*, edited by H. Misawa and S. Juodkazis, (Wiley, Weinheim, 2006).
[11] A. Vogel, J. Noack, G. Huttman, and G. Paltauf, Appl. Phys. B: Lasers Opt. **81**, 1015 (2005).
[12] S. Gaspard, M. Forster, C. Huber, C. Zafiu, G. Trettenhahn, W. Kautek, and M. Castillejo, Phys. Chem. Chem. Phys. **10**, 6174 (2008).
[13] H. Lubatschowski and A. Heisterkamp, in *Femtosecond Technology for Technical and Medical Applications*, edited by F. Dausinger, F. Lichtner, and H. Lubatschowski; *Topics of Applied Physics* (Springer, Berlin/Heidelberg, 2004) Vol. 96, p. 91.
[14] A. Vogel, N. Linz, S. Freidank, and G. Paltauf, Phys. Rev. Lett. **100**, 038102 (2008).
[15] E. G. Gamaly, S. Judokazis, K. Nishimura, and H. Misawa, Phys. Rev. B **73**, 214101 (2006).
[16] R. R. Gattass and E. Mazur, Nat. Photonics **2**, 219 (2008).
[17] Y. Liu, S. Sun, S. Sinha, M. R. Cho, and R. J. Gordon, Biomaterials **26**, 4597 (2005).
[18] S. Gaspard, M. Oujja, R. de Nalda, C. Abrusci, F. Catalina, L. Bañares, and M. Castillejo, Appl. Surf. Sci. **253**, 642 (2007).
[19] S. Gaspard, M. Oujja, R. de Nalda, M. Castillejo, L. Bañares, S. Lazare, and R. Bonneau, Appl. Phys. A: Mater. Sci. Process. **93**, 209 (2008).
[20] V. M. Correlo, L. F. Boesel, M. Bhattacharya, J. F. Mano, N. M. Neves, and R. L. Reis, Mater. Sci. Eng., A **403**, 57 (2005).
[21] M. F. A. Goosen, *Applications of Chitin and Chitosan* (Technomic, Pennsylvania, 1997).
[22] A. Sionkowska, J. Kozłowska, A. Płanecka, and J. Skopinska-Wisniewska, Appl. Surf. Sci. **255**, 2030 (2008).
[23] K. Sakurai, T. Maegawa, and T. Takahashi, Polymer **41**, 7051 (2000).
[24] J. B. Ashcom, R. R. Gattass, C. B. Schaffer, and E. Mazur, J. Opt. Soc. Am. B **23**, 2317 (2006).
[25] E. T. J. Nibbering, M. A. France, B. S. Prade, C. Grillon, C. Le Blanc, and A. Mysyrowicz, Opt. Commun. **119**, 479 (1995).
[26] C. Abrusci, A. Martín-González, A. Del Amo, F. Catalina, P. Bosch, and T. Corrales, J. Photochem. Photobiol., A **163**, 537 (2004).
[27] A. Bigi, S. Panzavolta, and K. Rubini, Biomaterials **25**, 5675 (2004).
[28] A. Sionkowska, in *Current Topics in Polymer Research, R*, edited by K. Bregg (Nova Science, New York, 2005), pp. 125–168.
[29] E. N. Glezer and E. Mazur, Appl. Phys. Lett. **71**, 882 (1997).
[30] S. Gaspard, M. Oujja, C. Abrusci, F. Catalina, S. Lazare, J. P. Desvergne, and M. Castillejo, J. Photochem. Photobiol., A **193**, 187 (2008).
[31] C. B. Schaffer, A. O. Jamison, and E. Mazur, Appl. Phys. Lett. **84**, 1441 (2004).